Received: 15 September 2020 | Revised: 1 December 2020 | Accepted: 3 January 2021

DOI: 10.1111/clr.13709

ORIGINAL RESEARCH

CLINICAL ORAL IMPLANTS RESEARCH WILEY

Assessment of soft and hard tissue dimensions following different treatment approaches of ligature-induced peri-implantitis defects

Ausra Ramanauskaite[1] | Karina Obreja[1] | Robert Sader[2] | Jürgen Becker[3] | Frank Schwarz[1]

[1]Department of Oral Surgery and Implantology, Goethe University, Carolinum, Frankfurt, Germany

[2]Department for Oral, Cranio-Maxillofacial and Facial Plastic Surgery, Medical Center of the Goethe University Frankfurt, Frankfurt am Main, Germany

[3]Department of Oral Surgery, Universitätsklinikum Düsseldorf, Düsseldorf, Germany

Correspondence
Frank Schwarz, Department of Oral Surgery and Implantology, Goethe University, Carolinum, Frankfurt, Germany.
Email: f.schwarz@med.uni-frankfurt.de

Abstract

Objectives: To evaluate peri-implant tissue dimensions following nonsurgical (NS) and surgical therapy (S) employing different decontamination protocols of advanced ligature-induced peri-implantitis in dogs.

Material & Methods: Peri-implantitis defects ($n = 5$ dogs, $n = 30$ implants) were randomly and equally allocated in a split-mouth design to NS or S treatment using either an Er:YAG laser (ERL), an ultrasonic device (VUS), or plastic curettes + local application of metronidazole gel (PCM), respectively. Horizontal bone thickness (hBT) and soft tissue thickness (hMT) were measured at different reference points: (v0) at the marginal portion of the peri-implant mucosa (PM); (v1) at 50% of the distance from PM to bone crest (BC); (v2) at the BC; (v3) at the most coronal extension of the bone-to-implant contact. Vertical peri-implant tissue height was calculated from PM to BC.

Results: All of the treatment groups showed a gradual hMT increase from v0 to the v2 reference point, followed by a reduction from v2 to the v3 region. The S-VUS subgroup tended to be associated with higher hMT values at the v0 region than the NS-VUS subgroup (0.44 mm versus 0.31 mm). PM-BC distance varied from 2.22 to 2.83 mm in the NS group, and from 2.07 to 2.38 in the S group.

Conclusion: Vertical and horizontal peri-implant tissue dimensions were similar in different treatment groups.

KEYWORDS

animal experiments, bone, dental implant, peri-implantitis treatment, soft tissue

1 | INTRODUCTION

Peri-implantitis is defined as a pathological condition that affects the tissues surrounding dental implants, characterized by an inflammation of the peri-implant mucosa and a subsequent progressive loss of supporting bone (Berglundh et al., 2018). Considerable evidence supports the microbial etiology of peri-implantitis, implicating that suppressing the progression of the disease requires removing bacterial plaque biofilms from the infected implant surfaces (Berglundh et al., 2018).

Implant surface decontamination can be accomplished through either nonsurgical or surgical approaches. Over the last several decades, numerous implant surface decontamination protocols of varying effectiveness have been advocated for peri-implantitis treatment. In fact, preclinical data indicated a lower apical extension of inflammatory cell infiltrates at implant sites treated with an erbium-doped: yttrium, aluminum, and garnet (Er:YAG) laser via a nonsurgical approach compared to those treated with an ultrasonic device or plastic curettes with adjunctive local antibiotics (Schwarz et al., 2006). Furthermore, Er:YAG laser decontamination performed via a surgical approach resulted in higher rates of re-osseointegration compared to those treated with the aforementioned measures (Schwarz et al., 2006).

From a clinical perspective, various nonsurgical peri-implantitis treatment strategies employing mechanical debridement alone or with adjunctive (i.e., local antibiotics or antimicrobial photodynamic therapy) and/or alternative measures (e.g., air abrasive devices or Er:YAG laser monotherapy) have demonstrated unpredictable treatment outcomes, largely attributable to limited access to the implant surface (Klinge & Meyle, 2012; Schwarz et al., 2015). On the contrary, surgical techniques that allow for direct access to the contaminated implant surface have shown clinical superiority in arresting disease progression (Schwarz et al., 2015). Nonetheless, recent recommendations also emphasize the need to assess the changes in peri-implant soft-tissue levels that, in turn, are essential for esthetic and biological outcomes of implant therapy (Giannobile et al., 2018; Jepsen et al., 2019).

Previous clinical data have demonstrated that diseased implant sites are associated with increased horizontal tissue thickness (Schwarz et al., 2017). Consequently, it appears to be reasonable that soft tissue-level changes following peri-implantitis therapy occur mainly due to a decrease in mucosal thickness as a result of the resolution of inflammatory soft-tissue infiltrates and, to a certain extent, trauma caused by surgical intervention.

The potential influence of various treatment procedures and decontamination methods on the dimensions of peri-implant tissues has not been addressed so far. In this context, it might be hypothesized that the invasiveness of therapeutic interventions, as well as decontamination protocols, may be associated with a different dimensional structure of peri-implant tissues. Therefore, the present study aims to evaluate peri-implant hard- and soft-tissue dimensions following nonsurgical and surgical therapy for advanced ligature-induced peri-implantitis using different implant surface decontamination protocols.

2 | MATERIALS AND METHODS

2.1 | Study design and animals

This study reports on a supplementary histological analysis of tissue biopsies obtained from previous experimental study employing a total of five 6-year-old female beagle dogs (mean weight 16.3 kg) (Schwarz et al., 2006). During the experiment, the dogs were fed once per day with soft-food diet and water. Animal selection, management, and surgery protocol were approved by the local authority (Animal Care and Use Committee of the Heinrich Heine University and the Bezirksregierung Düsseldorf) and the present reporting followed the ARRIVE Guidelines.

2.2 | Anesthesia protocol and experimental procedures

The anesthesia/analgesia protocols and experimental procedures have been detailed previously (Schwarz et al., 2006). In brief, after intramuscular sedation with acepromazine (0.17 mg/kg of body weight; Vetranquil 1%, Ceva Tiergesundheit, Düsseldorf, Germany), the dogs were anesthetized with 21.5 mg/kg thiopental sodium (Traoanal 2.5%, Altana GmbH, Konstanz, Germany). For all surgical procedures, inhalation anesthesia was performed by the use of oxygen and nitrous oxide and isoflurane. To maintain hydration, all animals received a constant infusion rate of lactated Ringer's solution while anesthetized. The experimental phases included the following procedures:

Phase 1 (*Tooth extraction*): After reflection of the full-thickness mucoperiosteal flaps and tooth separation, P2-M1 were carefully removed. Wound closure was performed by means of mattress sutures, and the sites were allowed to heal for 4 months.

Phase 2 (*Implant placement*): Following the elevation of the full-thickness mucoperiosteal flaps, three sand-blasted, large grit, and acid-etched (SLA) titanium implants were epicrestally placed on each side of the mandible (narrow neck, ∅ 3.3 mm, length 10 mm, Institut Straumann® AG) ($n = 6$ implants per dog) at 8 mm apart. All implants were connected with healing abutments (height: 2 mm, Institut Straumann® AG) and left to heal for 3 months in a transmucosal position.

Phase 3 (*Induction of Peri-implantitis*): Peri-implant mucosal inflammation was initiated by the submucosal placement of cotton ligatures (4–0) around each implant (Lindhe et al., 1992), and the plaque control regimen was terminated.

Phase 4 (*Progression of ligature-induced Peri-implantitis*): The ligatures were replaced once every 3 weeks and removed when approximately 40% of the initial bone support was lost (approximately 3 months), based on standardized radiographs. This was followed by a progression period of 4 weeks.

Phase 5 (*Peri-implantitis Treatment*): At the end of the progression period and renewal of the plaque control regimen, defects were randomly and equally allocated in a split-mouth design either as nonsurgical submucosal instrumentation (NS) or as access flap surgery (S) using one of the following debridement/decontamination approaches (Figure 1):

- Er: YAG laser treatment (KEY3®; KaVo; 100 mJ/pulse, 10 Hz, and pulse energy at the tip was approximately 85 mJ/pulse) (ERL).

- Ultrasonic device with a straight polyether ether ketone fiber (PEEK) and a polishing fluid (HA particles <10 μm) (Vector®; Dürr) (VUS).
- Plastic curettes (Institut Straumann AG), followed by subgingival (i.e., CNS- groups) or peri-implant application of metronidazole gel 25% (in S groups; Elyzol®; Colgate-Palmolive) (PCM).

Accordingly, the following treatment subgroups were tested in each animal ($n = 5$)1:

- NS-ERL
- NS-VUS
- NS-PCM
- S-ERL
- S-VUS
- S-PCM

All implant sites in S group underwent a submerged healing. Implants in the NS group were left to heal in a transmucosal position.

3 | CLINICAL MEASUREMENTS

Changes of mucosal recession (deltaMRb) at the vestibular aspect were assessed for the implants in the NS group at the baseline (i.e., before the ligature placement) and 3 months after treatment. The measurements from the implant shoulder (IC) to the mucosal margin (PM) were performed by using the PCP12 periodontal probe.

3.1 | Histological preparation

The animals were sacrificed (overdose of sodium pentobarbital 3%) after a healing period of 3 months, and the oral tissues were fixed by perfusion with 10% buffered formalin administered through the carotid arteries. The histological preparation has been reported in detail previously (Schwarz et al., 2006). In brief, the tissue biopsies were dehydrated using ascending grades of alcohol and xylene, infiltrated, and embedded in methyl methacrylate (MMA) (Technovit 9100 NEU; Heraeus Kulzer) for non-decalcified sectioning (Exakt®; Apparatebau). The most central section prepared at each implant site in the vestibulo-oral direction was ground to a final thickness of approximately 30 μm and stained with toluidine blue.

3.2 | Histological analysis

For image acquisition, a color CCD camera (Color View III; Olympus) was mounted on a binocular light microscope (Olympus BX50; Olympus). Digital images (original magnification × 200) were evaluated using a software program (analySIS FIVE docu®; Soft Imaging System).

The following landmarks were identified in the stained sections (Figure 2): PM, the bone crest (BC), the most coronal extension of the bone-to-implant contact (CBI). The horizontal mucosal thickness (hMT) and bone thickness (hBT) were the primary outcomes measured perpendicularly to the implant axis at the level of PM (v0), 50% IS-BC (v1), BC (v2), and CBI (v3). Vertical soft-tissue complex height was measured from PM to BC.

All histological measurements were performed by one calibrated examiner. The intra-examiner reproducibility was evaluated using 10 randomly selected histological specimens. The calculated mean variability between the repeated measurements at baseline and 48 hr was 0.940 ± 0.041.

3.3 | Statistical analysis

The statistical analysis of the data sets was accomplished using a commercially available software program (IBM SPSS Statistics 26.0; IBM Corp.).

Mean values, standard deviations, and medians were calculated for all parameters in different treatment groups defining the animal as statistical unit. Due to the low sample size and exploratory nature of the analysis, only descriptive statistics were applied.

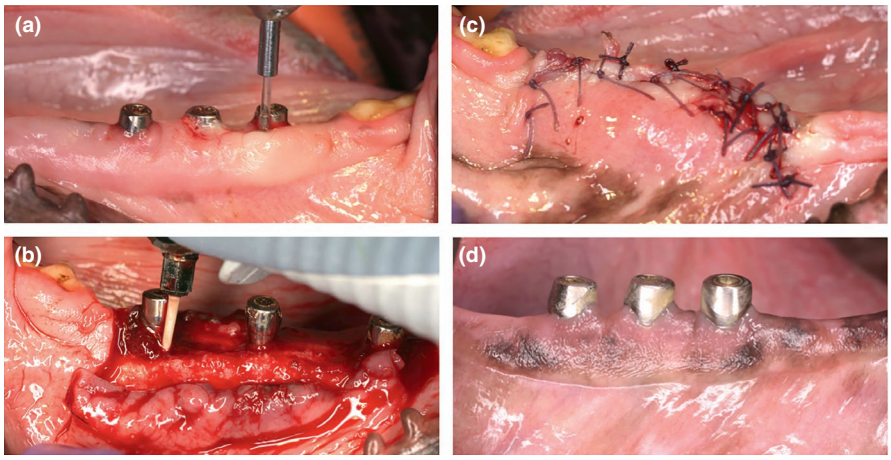

FIGURE 1 Peri-implantitis lesions were randomly and equally allocated in a split-mouth design to either nonsurgical treatment (NS) or access flap surgery (S) using different instrumentation methods: (a) NS using the Er: YAG laser treatment. (b) S using ultrasonic device. (c) Submerged healing following S approach. (d) Non-submerged healing following NS treatment

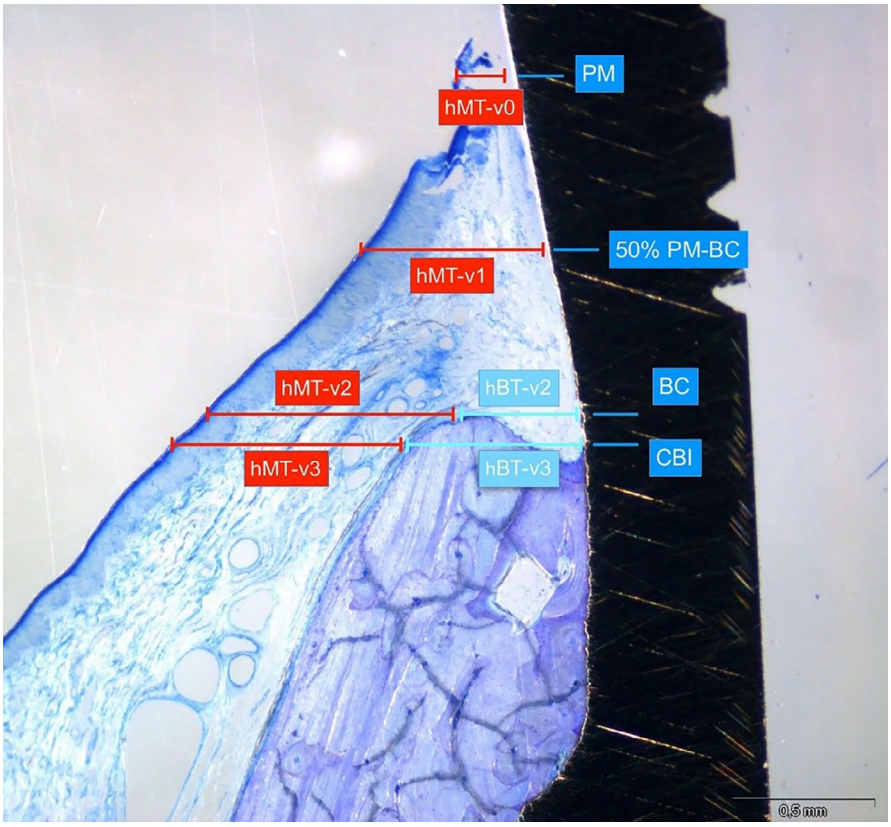

FIGURE 2 The following reference points served for the assessment of hMT (red lines) and hBT (turquois lines) values (specimen of the EB group): PM, peri-implant mucosal margin; BC, bone crest 50% PM-BC; CBI, coronal extension of bone-to-implant contact

4 | RESULTS

The postoperative healing was uneventful in all cases. However, all implant sites were exposed at between 8 and 10 weeks following primary wound closure in the S group.

Box plots indicating clinical and histological measurements in different treatment groups are depicted in Figure 3a,c. Clinically, mean values of deltaMRb in NS group ranged from 1.06 ± 0.61 mm to 2.06 ± 0.66 mm. In particular, the lowest values appeared in the NS-ERL subgroup, and the highest values were registered in the NS-PCM subgroup. The mean postoperative mucosal recession amounted to 1.10 ± 0.64 mm, 0.89 ± 1.12 mm, and 0.38 ± 1.19 mm for the S-ERL, S-VUS, and S-PCM subgroups, respectively.

Mean PM-BC values in the NS subgroup amounted to 2.22 ± 0.41 mm (NS-PCM), 2.49 ± 0.93 mm (NS-VUS), and 2.83 ± 1.16 mm (NS-ERL). Lower mean values were recorded in the S group for the VUS and ERL subgroups (S-PCM: 2.38 ± 0.31 mm, S-VUS: 2.07 ± 0.83 mm; S-ERL: 2.08 ± 0.47 mm).

All treatment groups showed a gradual hMT increase from v0 toward the v2 region, followed by a reduction from v2 to the v3 region. At the v0 region, the mean hMT ranged from 0.31 ± 0.069 mm to 0.35 ± 0.13 mm in NS groups and from 0.29 ± 0.13 mm to 0.44 ± 0.09 mm in the S groups. The mean hMT at the v0 reference point in the S-VUS subgroup tended to be higher compared to the NS-VUS subgroup (0.44 mm versus 0.31 mm). The mean estimated hMT increase from v0 to v2 reached 1.12 ± 0.16 mm in the NS-PCM subgroup, 1.51 ± 0.54 mm in the NS-ERL subgroup, and 1.61 ± 0.75 mm in the NS-VUS subgroup. The corresponding mean values in the S treatment subgroups were 1.22 ± 0.04 mm (S-PCM), 1.38 ± 0.38 mm (S-ERL), and 1.66 ± 0.19 mm (S-VUS), respectively. Regarding the v2-v3 hMT reduction, the PMS subgroup showed the smallest mean decrease in the NS and S groups (0.25 ± 0.09 mm and 0.24 ± 0.33 mm, respectively). These corresponded to 0.45 ± 0.36 mm and 0.60 ± 0.44 mm for the NS-VUS and S-VUS subgroups and to 0.67 ± 0.44 and 0.53 ± 0.35 mm for the NS-ERL and S-ERL subgroups, respectively.

In all treatment subgroups, the hBT increased from v2 to v3. For the NS groups, the mean hBT values ranged from 0.67 ± 0.16 mm to 0.85 ± 0.39 mm at the v2 area, and from 1.15 ± 0.46 mm to 1.85 ± 0.77 mm at the v3 area. A mean hBT increase from the v2 to v3 reference point of 0.48 ± 0.29 and 0.58 ± 0.23 mm was registered for the NS-VUS and NS-PMS subgroups, respectively, while the highest mean hBT increase occurred in the NS-ERL subgroup (1.0 ± 0.45 mm). For the S treatment subgroups, hBT values ranged from 0.61 ± 0.32 mm to 0.81 ± 0.04 mm at the v2 reference point, and from 1.21 ± 0.02 to 1.65 ± 0.48 mm in the v3 region. The mean hMT increase from v2 to the v3 region was 0.56 ± 0.21 mm in the S-PMC subgroup, 0.84 ± 0.44 mm in the S-ERL subgroup, and 1.08 ± 0.64 mm in the S-VU subgroup.

5 | DISCUSSION

The present analysis was aimed at assessing vertical and horizontal peri-implant tissue dimensions following nonsurgical and surgical therapies employing different decontamination protocols of advanced ligature-induced peri-implantitis in a canine model.

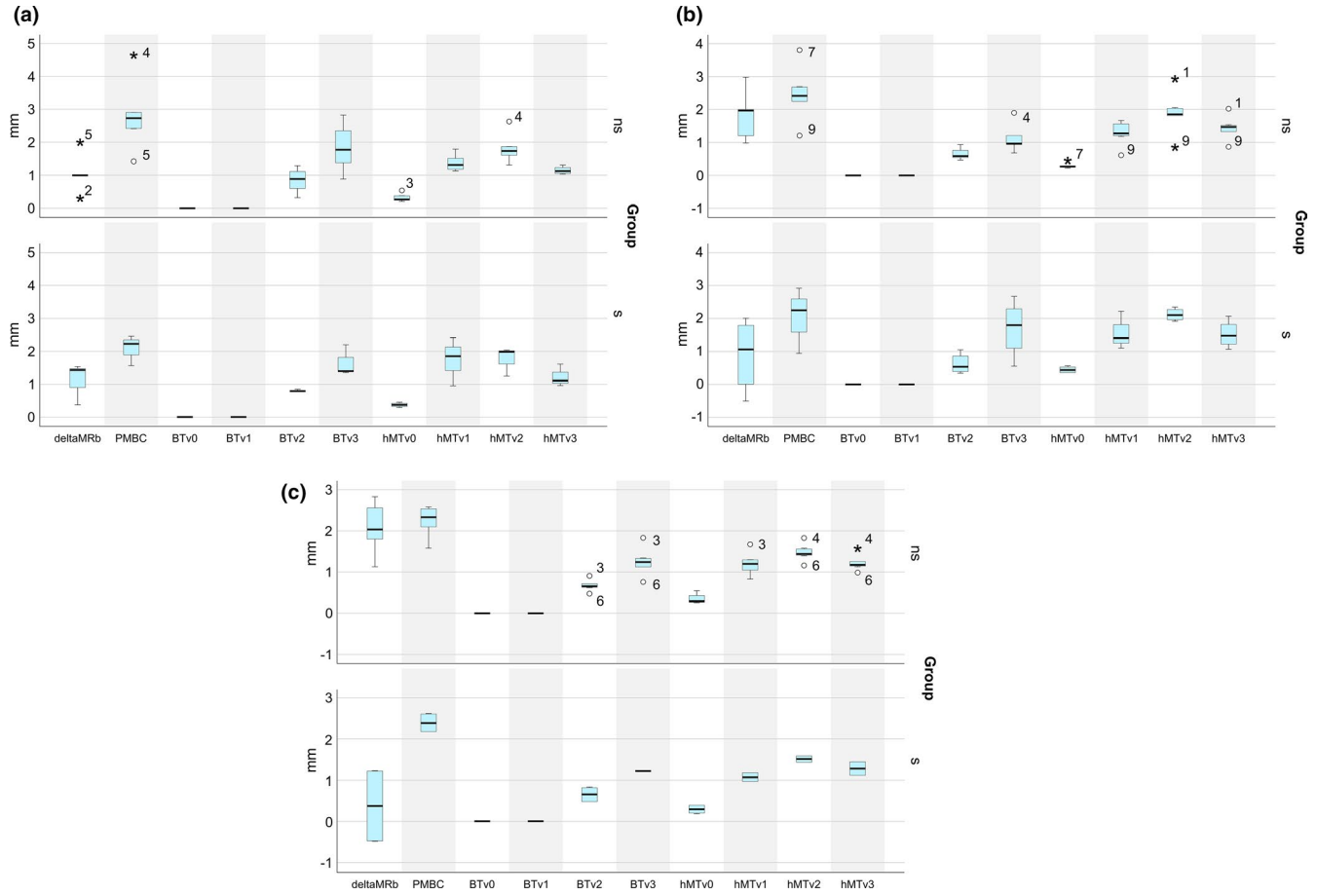

FIGURE 3 Boxplots indicating deltaMRb (delta just refers to the ns group), PM-BC, hMT, and hBT values in different treatment groups: (a) ERL. (b) VUS. (c) PCM

Based on the histological findings, mean vertical soft-tissue dimensions tended to be slightly higher in the NS treatment groups, compared to those assessed in S groups (NS range: 2.22–2.83 mm; S range: 2.07–2.38 mm), suggesting that a non-invasive therapeutic approach may facilitate the preservation of vertical soft-tissue height. Generally, the detected vertical mucosal height is within the range of those reported in previous preclinical investigations in dogs, in which junctional epithelial and underlying connective tissue height ranged from 1.64 to 2.35 mm and from 0.50 to 1.80 mm, respectively (Abrahamsson et al., 1996, 1999; Berglundh & Lindhe, 1996, 1997). It is worth noting that a previous analysis of the present data set revealed a significantly longer epithelial junction for the implant sites in the S groups that underwent submerged postoperative healing, compared to those measured in the NS groups (i.e., non-submerged healing), thereby corroborating the observations of prior studies of canine models (Abrahamsson et al., 1999; Hermann et al., 2001). However, the opposing data indicated that healing pattern did not affect vertical mucosal height (Weber et al., 1996). To the authors' best knowledge, these are the first data on the soft-tissue dimensions at peri-implantitis sites following different surgical treatment strategies.

Further analysis of horizontal soft-tissue dimensions revealed a pattern of consistent hMT increases from the IS toward BC in both treatment groups, which aligns with the results of a previous preclinical study (Schwarz et al., 2016). Accordingly, the lowest mean hMT values in all subgroups were assessed in the IS area (NS range: 0.31–0.35 mm; S range: 0.29–0.44 mm). In the VUS group, there was a tendency of higher hMT values in S-VUS subgroup at IS compared to the NS-VUS subgroup (0.44 mm versus 0.31 mm, respectively). The highest measurements were registered in the BC region, with a tendency toward slightly superior hMT dimensions in the S group (NS range of mean values: 1.47–1.91 mm; S range: 1.51–2.10 mm). In this context, it is worth noticing that the greatest mean hMT increase in the apical direction was registered in the NS-VUS and S-ERL subgroups (1.60 and 1.66 mm, respectively), which, based on a previous analysis of the present data, showed the highest apical extension of the inflammatory cell infiltrate (1.6 and 1.4 mm, respectively), thus indicating that the extent of residual inflammatory infiltrate might be associated with hMT (Schwarz et al., 2006). The latter tendency may be at least in part supported by the former clinical data, which demonstrated a significant increase in hMT in the presence of peri-implant tissue inflammation, compared to healthy implant sites (Schwarz et al., 2017).

When further considering horizontal hard tissue dimensions, the general pattern indicated an increase in hBT in the apical direction (i.e., toward the v3 reference point) in all treatment subgroups. Given

the previously reported analysis of the present data set, an opposing tendency to that noted for hMT could be observed for hBT, suggesting that reduced apical extension of inflammatory cell infiltrate tended to be associated with the greater mean hBT increase in the apical direction leading to the higher hBT dimensions at the v3 reference point (Schwarz et al., 2006). In particular, in the NS group, the most pronounced mean hBT increase and the highest hBT values were registered for the ERL followed by PCM subgroups, which in turn presented with the lowest inflammatory tissue extension apically (NS-ERL: 0.9 mm; NS-PCM: 1.3 mm; NS-VUS: 1.6 mm) (Schwarz et al., 2006). Likewise, in the S group, VUS subgroup showed the lowest apical extension of inflammatory cell infiltrate (S-VUS: 1.0 mm; S-ERL: 1.4 mm; S-PCM: 1.3 mm), which subsequently was associated with the largest increase in mean hBT and the highest hBT values in the v3 area (Schwarz et al., 2006).

Recent clinical data demonstrated that mucosal recession is not a rare finding (31%) at implant sites affected by peri-implantitis (Obreja et al., 2020). Furthermore, peri-implantitis therapy has been shown to be frequently associated with soft-tissue recession (Heitz-Mayfield et al., 2018; Matarasso et al., 2014; Romeo et al., 2007; Roos-Jansåker et al., 2007). Corroborating the clinical data, the mean mucosal recession in the present analysis measured at baseline (i.e., prior to initiation of inflammation) and after the treatment in the NS group ranged from 1.6 to 2.06 mm. In the S group, all implant sites were primarily exposed during the healing phase, allowing for an assessment of mucosal recession, which mean values ranged between 0.38 and 1.10 mm. In this context, however, it was impossible to determine the extent to which the recession in the NS group related to the occurrence of tissue inflammation and the extent to which it was a consequence of the treatment. Moreover, due to the different healing patterns (i.e., submerged versus. non-submerged), it was not feasible to compare mucosal recession values between NS and S groups.

Upon the results of the present analysis, the method of implant surface decontamination seemed to have an impact on horizontal soft- and hard-tissue dimensions. When interpreting the aforementioned findings, it is important to remark that, in the clinical setting, NS treatment irrespective of the decontamination protocol showed limited efficacy (Schwarz et al., 2015). Surgical approaches, by contrast, have demonstrated superiority in arresting peri-implantitis progression without prioritizing any particular implant surface decontamination method (Koo et al., 2019; Schwarz et al., 2015). The clinical relevance of different decontamination protocols on tissue dimensional changes needs to be further elaborated.

The present analysis represents secondary outcomes of the previous study, in which the original protocol was aimed primarily at assessing the effectiveness of different treatment approaches for experimentally induced peri-implantitis lesions. Therefore, hypothesis testing was not feasible and only descriptive analyses were applied. Furthermore, comparing the different healing patterns (i.e., submerged and non-submerged) may, to some extent, have influenced the outcomes of the analysis. Nonetheless, during the healing phase, all implant sites in the submerged healing group were exposed, which makes the results comparable between the S and NS groups. Finally, it is worth noting that one recent experimental analysis demonstrated that implant macrodesign affected the bone-loss rates following the peri-implantitis induction phase, favoring bone-level implants with a platform-switching design over regular neck tissue-level implants (Sanz-Esporrin et al., 2020). Therefore, one might speculate that the implant design used in the present analysis (i.e., tissue-level narrow-neck implants) might have affected the extent of peri-implantitis lesions and subsequently the treatment outcomes, at least to some certain extent.

Within its limitations, the present analysis has pointed to a tendency toward similar vertical and horizontal peri-implant tissue dimensions in different treatment groups and subgroups.

ACKNOWLEDGEMENTS

The study was self-funded by the authors own departments. The original study protocol was funded by a grant of the "DGI—Deutsche Gesellschaft für Implantologie im Zahn-, Mund- und Kieferbereich."

CONFLICT OF INTEREST

All authors stated explicitly that there are no conflicts of interest related to this article.

AUTHOR CONTRIBUTION

Ausra Ramanauskaite contributed to the data acquisition, interpretation and analysis, and manuscript writing; Karina Obreja contributed to the data acquisition and interpretation; Robert Sader and Jürgen Becker contributed to data analysis and critical revision of the manuscript; Frank Schwarz contributed to idea generation, conception, and interpretation of data, manuscript writing, and critical revision.

DATA AVAILABILITY STATEMENT

Data openly available in a public repository that does not issue DOIs.

ORCID

Ausra Ramanauskaite https://orcid.org/0000-0002-1649-1882
Frank Schwarz https://orcid.org/0000-0001-5515-227X

REFERENCES

Abrahamsson, I., Berglundh, T., Moon, I. S., & Lindhe, J. (1999). Peri-implant tissues at submerged and non-submerged titanium implants. *Journal of Clinical Periodontology*, *26*, 600–607. https://doi.org/10.1034/j.1600-051X.1999.260907.x

Abrahamsson, I., Berglundh, T., Wennström, J., & Lindhe, J. (1996). The peri-implant hard and soft tissues at different implant systems. A comparative study in the dog. *Clinical Oral Implants Research*, *7*, 212–219. https://doi.org/10.1034/j.1600-0501.1996.070303.x

Berglundh, T., Armitage, G., Araujo, M. G., Avila-Ortiz, G., Blanco, J., Camargo, P. M., Chen, S., Cochran, D., Derks, J., Figuero, E., Hämmerle, C. H. F., Heitz-Mayfield, L. J. A., Huynh-Ba, G., Iacono, V., Koo, K. T., Lambert, F., McCauley, L., Quirynen, M., Renvert, S., … Zitzmann, N. (2018). Peri-implant diseases and conditions: Consensus report of workgroup 4 of the 2017 World Workshop on the Classification of Periodontal and Peri-Implant Diseases and Conditions. *Journal of Periodontology*, *89*(Suppl 1), S313–S318.

Berglundh, T., & Lindhe, J. (1996). Dimension of the periimplant mucosa. *Biological Width Revisited Journal of Clinical Periodontology*, *23*, 971–973. https://doi.org/10.1111/j.1600-051X.1996.tb00520.x

Berglundh, T., & Lindhe, J. (1997). Healing around implants placed in bone defects treated with Bio-Oss. *An Experimental Study in the Dog Clinical Oral Implants Research*, *8*, 117–124. https://doi.org/10.1034/j.1600-0501.1997.080206.x

Giannobile, W. V., Jung, R. E., & Schwarz, F. (2018). Evidence-based knowledge on the aesthetics and maintenance of peri-implant soft tissues: Osteology Foundation Consensus Report Part 1-Effects of soft tissue augmentation procedures on the maintenance of peri-implant soft tissue health. *Clinical Oral Implants Research*, *29*(Suppl 15), 7–10. https://doi.org/10.1111/clr.13110

Heitz-Mayfield, L. J. A., Salvi, G. E., Mombelli, A., Loup, P. J., Heitz, F., Kruger, E., & Lang, N. P. (2018). Supportive peri-implant therapy following anti-infective surgical peri-implantitis treatment: 5-year survival and success. *Clinical Oral Implants Research*, *29*, 1–6. https://doi.org/10.1111/clr.12910

Hermann, J. S., Cochran, D. L., Hermann, J. S., Buser, D., Schenk, R. K., & Schoolfield, J. D. (2001). Biologic Width around one- and two-piece titanium implants. *Clinical Oral Implants Research*, *12*, 559–571. https://doi.org/10.1034/j.1600-0501.2001.120603.x

Jepsen, S., Schwarz, F., Cordaro, L., Derks, J., Hämmerle, C. H. F., Heitz-Mayfield, L. J., Hernández-Alfaro, F., Meijer, H. J. A., Naenni, N., Ortiz-Vigón, A., Pjetursson, B., Raghoebar, G. M., Renvert, S., Rocchietta, I., Roccuzzo, M., Sanz-Sánchez, I., Simion, M., Tomasi, C., Trombelli, L., & Urban, I. (2019) Regeneration of alveolar ridge defects. Consensus report of group 4 of the 15th European Workshop on Periodontology on Bone Regeneration. *Journal of Clinical Periodontology*, *46*(Suppl 21), 277–286.

Klinge, B., & Meyle, J. (2012). Peri-implant tissue destruction. The Third EAO Consensus Conference 2012. *Clinical Oral Implants Research*, *23*(Suppl 6), 108–110.

Koo, K. T., Khoury, F., Keeve, P. L., Schwarz, F., Ramanauskaite, A., Sculean, A., & Romanos, G. (2019). Implant surface decontamination by surgical treatment of periimplantitis: A literature review. *Implant Dentistry*, *28*, 173–176. https://doi.org/10.1097/ID.0000000000000840

Lindhe, J., Berglundh, T., Ericsson, I., Liljenberg, B., & Marinello, C. (1992). Experimental breakdown of peri-implant and periodontal tissues. *A Study in the Beagle Dog Clinical Oral Implants Research*, *3*, 9–16. https://doi.org/10.1034/j.1600-0501.1992.030102.x

Matarasso, S., Iorio Siciliano, V., Aglietta, M., Andreuccetti, G., & Salvi, G. E. (2014). Clinical and radiographic outcomes of a combined resective and regenerative approach in the treatment of peri-implantitis: A prospective case series. *Clinical Oral Implants Research*, *25*, 761–767. https://doi.org/10.1111/clr.12183

Obreja, K., Ramanauskaite, A., Begic, A., Galarraga-Vinueza, M. E., Sader, R., & Schwarz, F. (2020). The prevalence of peri-implant diseases for subcrestally inserted implants: A cross sectional study. Clin Oral Implants Res. Under revision.

Romeo, E., Lops, D., Chiapasco, M., Ghisolfi, M., & Vogel, G. (2007). Therapy of peri-implantitis with resective surgery. A 3-year clinical trial on rough screw-shaped oral implants. *Part II: Radiographic Outcome Clinical Oral Implants Research*, *18*, 179–187.

Roos-Jansåker, A. M., Renvert, H., Lindahlmn, C., & Renvert, S. (2007). Surgical treatment of peri-implantitis using a bone substitute with or without a resorbable membrane: A prospective cohort study'. *Journal of Clinical Periodontology*, *34*, 625–632. https://doi.org/10.1111/j.1600-051X.2007.01102.x

Sanz-Esporrin, J., Carral, C., Blanco, J., Sanz-Casado, J. V., Muñoz, F., & Sanz, M. (2020). Differences in the progression of experimental peri-implantitis depending on the implant to abutment connection. *Clinical Oral Investigations*, https://doi.org/10.1007/s00784-020-03680-z

Schwarz, F., Claus, C., & Becker, K. (2017). Correlation between horizontal mucosal thickness and probing depths at healthy and diseased implant sites. *Clinical Oral Implants Research*, *28*, 1158–1163. https://doi.org/10.1111/clr.12932

Schwarz, F., Jepsen, S., Herten, M., Sager, M., Rothamel, D., & Becker, J. (2006). Influence of different treatment approaches on non-submerged and submerged healing of ligature induced peri-implantitis lesions: An experimental study in dogs. *Journal of Clinical Periodontology*, *33*, 584–595. https://doi.org/10.1111/j.1600-051X.2006.00956.x

Schwarz, F., Sager, M., Golubovic, V., Iglhaut, G., & Becker, K. (2016). Horizontal mucosal thickness at implant sites as it correlates with the integrity and thickness of the buccal bone plate. *Clinical Oral Implants Research*, *27*, 1305–1309. https://doi.org/10.1111/clr.12747

Schwarz, F., Schmucker, A., & Becker, J. (2015). Efficacy of alternative or adjunctive measures to conventional treatment of peri-implant mucositis and peri-implantitis: A systematic review and meta-analysis. *International Journal of Implant Dentistry*, *1*, 22. https://doi.org/10.1186/s40729-015-0023-1

Weber, H. P., Buser, D., Donath, K., Fiorellini, J. P., Doppalapudi, V., Paquette, D. W., & Williams, R. C. (1996). Comparison of healed tissues adjacent to submerged and non-submerged unloaded titanium dental implants. A histometric study in beagle dogs. *Clinical Oral Implants Research*, *7*, 11–19. https://doi.org/10.1034/j.1600-0501.1996.070102.x

How to cite this article: Ramanauskaite A, Obreja K, Sader R, Becker J, Schwarz F. Assessment of soft and hard tissue dimensions following different treatment approaches of ligature-induced peri-implantitis defects. *Clin Oral Impl Res*. 2021;32:394–400. https://doi.org/10.1111/clr.13709